Disclination asymmetry in two-dimensional nematic liquid crystals with unequal Frank constants

Michael W. Deem
Chemical Engineering Department, University of California, Los Angeles, California 90095-1542
(Received 19 June 1996)

The behavior of a thin film of nematic liquid crystal with unequal Frank constants is discussed. Distinct Frank constants are found to imply unequal core energies for $+1/2$ and $-1/2$ disclinations. Even so, a topological constraint is shown to ensure that the bulk densities of the two types of disclinations are the same. For a system with free boundary conditions, such as a liquid membrane, unequal core energies simply renormalize the Gaussian rigidity and line tension. [S1063-651X(96)06712-8]

PACS number(s): 61.30.−v

I. INTRODUCTION

This paper discusses the disclination-mediated isotropic-ordered transition in a thin film of nematic liquid crystal. The focus is on the case where the bend and splay Frank constants are distinct. The free energy of this system is given to lowest order by [1]

$$H=\frac{k_1}{2}\int dx\,dy[\nabla\cdot\mathbf{n}(x,y)]^2+\frac{k_3}{2}\int dx\,dy|\nabla\times\mathbf{n}(x,y)|^2. \tag{1}$$

Here $\mathbf{n}$ is the orientation of the nematic molecule and is of unit length. This free energy can alternatively be expressed in terms of the orientation of the molecules as

$$H=\frac{J}{2}\int dx\,dy(\theta_x^2+\theta_y^2)+\frac{\Delta}{2}\int dx\,dy\cos(2\theta)(\theta_y^2-\theta_x^2)$$
$$-\Delta\int dx\,dy\sin(2\theta)\theta_x\theta_y, \tag{2}$$

where $J=(k_1+k_3)/2$, $\Delta=(k_1-k_3)/2$, and the subscripts denote derivatives. If the two Frank constants were equal, this free energy would simply be that of the X-Y model. For the symmetric nematics considered here, however, the natural defects are $\pm1/2$ disclinations rather than the ±1 disclinations of the conventional X-Y model. It will be shown that the presence of nonzero Δ causes the ground-state energies of $\pm1/2$ disclinations to differ by $O(\Delta^2)$. The disclination energies diverge logarithmically in the system size, but with unequal coefficients. The elementary Kosterlitz-Thouless energy-entropy balance thus seems to lead to different proliferation temperatures for these defects. This famous argument [2] predicts that a $+1/2$ or $-1/2$ defect proliferates whenever the free energy to create a disclination, $F_{+1/2}(R)=E_{+1/2}(R)-2k_BT\ln(R/a_0)$ or $F_{-1/2}(R)=E_{-1/2}(R)-2k_BT\ln(R/a_0)$, becomes negative. Here $E_{+1/2}(R)$ and $E_{-1/2}(R)$ are disclination energies as a function of the system size R, and a_0 is a microscopic cutoff.

In fact, thermal fluctuations of the nematics drive the two Frank constants to the same value at long wavelengths, so that there is a unique Kosterlitz-Thouless transition temperature. The essential effect of nonzero Δ is to create a distinct long-ranged contribution to the core energy of each defect. For a system above the isotropic-ordered transition, this difference in core energies can be substantial and would seem to lead to different densities of $+1/2$ and $-1/2$ disclinations. As the correlation length grows near the isotropic-ordered transition, the core energy becomes negligible compared to the logarithmically diverging piece, and the disclinations pair into dislocations. At the transition, the densities of $+1/2$ and $-1/2$ disclinations must both become equal to the density of dislocations. In fact, Green's theorem implies that under all conditions the difference between the number of $+1/2$ and $-1/2$ disclinations can scale at most as the circumference of the system. The natural way for this to happen is $n_{+1/2}-n_{-1/2}\sim cR/\xi$, where ξ is the correlation length, and the prefactor depends on difference of exponentials of core energies. This constraint implies that $\pm1/2$ disclinations occur with the same density in a large system.

The ground-state energies of $\pm1/2$ disclinations are derived in Sec. II. The energies are found to be logarithmically diverging with unequal prefactors. It is shown in Sec. III that these coefficients should renormalize to the same value at long wavelengths due to renormalization of Δ to zero. The free energies of $\pm1/2$ disclinations in the ordered phase are directly calculated by perturbation theory in Sec. IV, and the $\pm1/2$ disclinations are found to differ by a core energy contribution. An approximate calculation of the disclination density in the isotropic phase is described in Sec. V. The $\pm1/2$ disclinations are shown to occur with equal densities for large systems. In fact, the number asymmetry is shown to scale only linearly with the system size. This issue is explored in Sec. VI with Monte Carlo calculations on a lattice model. The disclination number asymmetry is indeed found to be proportional to the circumference of the system. Section VII concludes with a discussion of these results.

II. GROUND-STATE ENERGIES OF ±1/2 DISCLINATIONS

The ground-state energies of $\pm1/2$ disclinations in the Hamiltonian (2) will be logarithmically diverging in the size of the system. The coefficient in front of the logarithm is calculated in this section. The coefficient is determined solely by the properties of the θ field far from the disclination, vanishing if the θ field vanishes at infinity and diverg-

ing unless the θ field goes to a constant. The ground-state configuration, therefore, must have $\theta(r,\phi)\sim\theta(\phi)$ as $r\to\infty$. With this form, the energy is given by

$$H\sim H_0\ln(R/a_0) \quad \text{as} \quad R\to\infty, \tag{3}$$

with

$$H_0=\frac{1}{2}\int_0^{2\pi} d\phi\,\theta'^2(\phi)\{J+\Delta\cos[2\phi-2\theta(\phi)]\}. \tag{4}$$

A disclination of strength s is defined by

$$\theta(\phi)=s\phi+\frac{\Delta}{J}\theta_1(\phi), \tag{5}$$

where $\theta_1(\phi)$ is continuous. The condition of a ground-state geometry, without the assumption of rotational symmetry, can be written as

$$\frac{\delta F_0}{\delta\theta}=0=-J\nabla^2\theta+\Delta\sin(2\theta)(\theta_y^2-\theta_x^2+2\theta_{xy})+\Delta\cos(2\theta)\times(\theta_{xx}-\theta_{yy}+2\theta_x\theta_y). \tag{6}$$

This equation implies that

$$\theta=\theta_0+\frac{\Delta}{J}\theta_1+O(\Delta^2/J^2), \tag{7}$$

with

$$\nabla^2\theta_0=0,$$

$$\nabla^2\theta_1=\sin(2\theta_0)(\theta_{0y}^2-\theta_{0x}^2+2\theta_{0xy})+\cos(2\theta_0)\times(\theta_{0xx}-\theta_{0yy}+2\theta_{0x}\theta_{0y}). \tag{8}$$

These equations are solved by

$$\theta_0(\phi)=s\phi, \quad \theta_1(\phi)=\frac{(2-s)s\sin[2\phi(s-1)]}{4(1-s^2)} \tag{9}$$

for a disclination of strength s.

For $s=+1/2$, Eq. (9) simplifies to

$$\theta_1(\phi)=-\frac{3}{4}\sin\phi \tag{10}$$

and leads to an energy of

$$H_0=\frac{\pi J}{4}-\frac{9\pi\Delta^2}{32J}+O(\Delta^3/J^2). \tag{11}$$

Similarly, for $s=-1/2$, Eq. (9) simplifies to

$$\theta_1(\phi)=\frac{5}{36}\sin(3\phi) \tag{12}$$

and leads to an energy of

$$H_0=\frac{\pi J}{4}-\frac{25\pi\Delta^2}{288J}+O(\Delta^3/J^2). \tag{13}$$

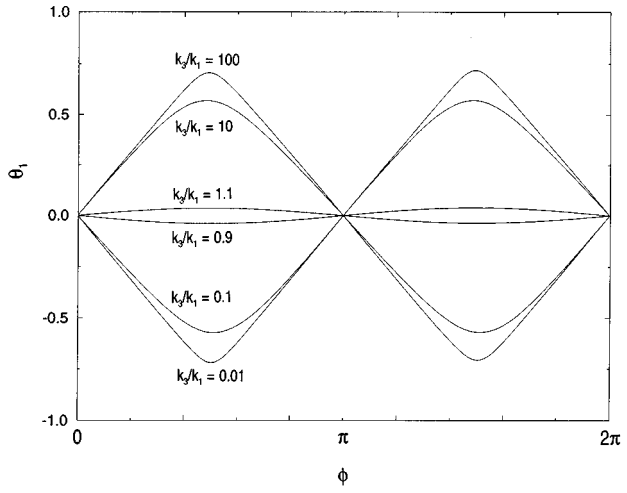

FIG. 1. θ versus ϕ for a $s=+1/2$ disclination.

The general result for the deviation field $\theta-\theta_0$ can be expressed in terms of elliptic integrals of the third kind [3]. Results for the angle field have been presented elsewhere [4]. To give the reader some feel for how larger values of Δ distort the ground-state geometry, the function $\theta(\phi)$ is shown for a $s=+1/2$ (Fig. 1) and a $s=-1/2$ (Fig. 2) disclination. These geometries were computed by defining $\theta(\phi)$ on a grid and numerically minimizing Eq. (4). Direct integration of Eq. (6) produced identical results. Extreme differences between the two Frank constants can substantially distort the $T=0$ geometries. Figure 3 shows the ground-state energies associated with different ratios of the Frank constants for $s=\pm 1/2$. One can see that the $s=+1/2$ disclination completely screens out either splay or bend as the associated Frank constant, k_1 or k_3, respectively, becomes large:

$$H_0\sim\pi k_3/2 \quad \text{as} \quad k_1\to\infty,$$

$$H_0\sim\pi k_1/2 \quad \text{as} \quad k_3\to\infty. \tag{14}$$

The $s=-1/2$ disclination, on the other hand, is unable to completely remove unfavorable bend or splay:

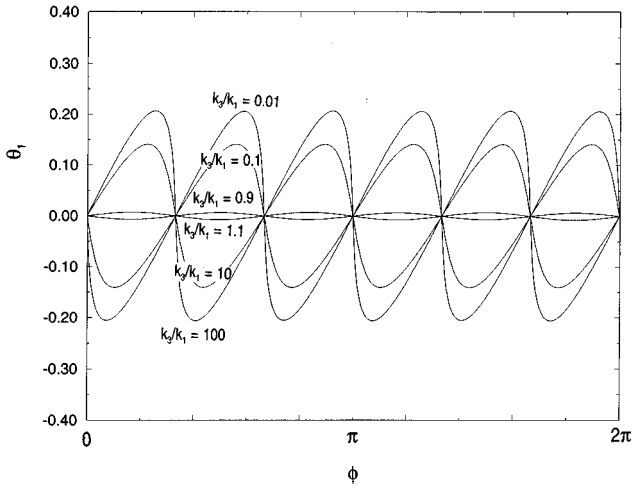

FIG. 2. θ versus ϕ for a $s=-1/2$ disclination.

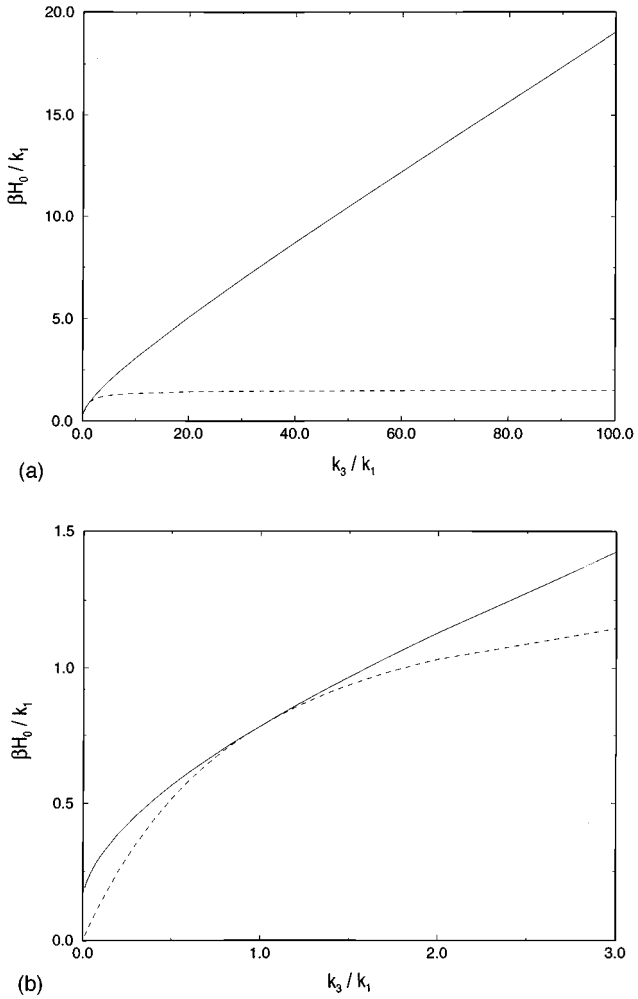

FIG. 3. E/J versus Δ for $s=+1/2$ (dashed line) and $s=-1/2$ (solid line).

$$H_0 \sim 0.191 k_1 \quad \text{as} \quad k_1 \to \infty,$$

$$H_0 \sim 0.191 k_3 \quad \text{as} \quad k_3 \to \infty. \tag{15}$$

III. RG FLOW EQUATION FOR Δ

The isotropic-ordered transition does not occur at $T=0$, and so it is the free energies of the two disclinations that should govern their densities in the isotropic phase. This issue is addressed here by looking at the renormalization of Δ due to thermal fluctuations around an isolated disclination.

For a $s=+1/2$ disclination the angle order parameter is expressed as

$$\theta(r,\phi) = \phi/2 + \psi(r,\phi). \tag{16}$$

The function $\psi(r,\phi)$ is single valued and smooth. The Hamiltonian (2) is expanded in powers of ψ, with the result

$$\begin{aligned} H[\psi] = {} & \frac{J}{2}\int \left(\frac{1}{4r^2} + \psi_x^2 + \psi_y^2 \right) + \frac{3\Delta}{4}\int \frac{y\psi}{r^3} \\ & + \frac{\Delta}{4}\int \left[-\frac{3x\psi^2}{r^3} + \frac{2x(\psi_y^2 - \psi_x^2)}{r} - \frac{4y\psi_x\psi_y}{r} \right] \\ & + \frac{\Delta}{6}\int \left[-\frac{3y\psi^3}{r^3} - \frac{6y\psi(\psi_y^2 - \psi_x^2)}{r} - \frac{12x\psi\psi_x\psi_y}{r} \right] \\ & + \frac{\Delta}{12}\int \left[\frac{3x\psi^4}{r^3} - \frac{12y\psi^2(\psi_y^2 - \psi_x^2)}{r} + \frac{24x\psi^2\psi_x\psi_y}{r} \right]. \end{aligned} \tag{17}$$

The renormalization of Δ is tracked by integrating out ψ on a momentum shell to first order in T/J and watching how terms from the ψ^3 expression contribute to terms in the ψ expression. The ψ expression can be written as

$$t_0 = \frac{3\pi i \Delta}{2}\int_{\mathbf{k}} \frac{k_y}{k}\hat{\psi}(-\mathbf{k}), \tag{18}$$

where $\int_{\mathbf{k}}$ means $\int d^2k/(2\pi)^2$. The ψ^3 expression can be broken down into

$$\begin{aligned} t_1 = {} & -\pi i \Delta \int_{\mathbf{k}_1\mathbf{k}_2\mathbf{k}_3\mathbf{k}_4} (2\pi)^2 \delta(\mathbf{k}_1+\mathbf{k}_2+\mathbf{k}_3+\mathbf{k}_4) \\ & \times \frac{k_{1y}}{k_1}\hat{\psi}(\mathbf{k}_2)\hat{\psi}(\mathbf{k}_3)\hat{\psi}(\mathbf{k}_4), \\ t_2 = {} & -2\pi i \Delta \int_{\mathbf{k}_1\mathbf{k}_2\mathbf{k}_3\mathbf{k}_4} (2\pi)^2 \delta(\mathbf{k}_1+\mathbf{k}_2+\mathbf{k}_3+\mathbf{k}_4) \\ & \times \frac{k_{1y}}{k_1^3}\hat{\psi}(\mathbf{k}_2)\hat{\psi}(\mathbf{k}_3)\hat{\psi}(\mathbf{k}_4)(k_{3x}k_{4x} - k_{3y}k_{4y}), \\ t_3 = {} & -4\pi i \Delta \int_{\mathbf{k}_1\mathbf{k}_2\mathbf{k}_3\mathbf{k}_4} (2\pi)^2 \delta(\mathbf{k}_1+\mathbf{k}_2+\mathbf{k}_3+\mathbf{k}_4) \\ & \times \frac{k_{1x}}{k_1^3}\hat{\psi}(\mathbf{k}_2)\hat{\psi}(\mathbf{k}_3)\hat{\psi}(\mathbf{k}_4)(-k_{3x}k_{4y}). \end{aligned} \tag{19}$$

The momenta in the shell $k_c - dk_c < k < k_c$ can then be integrated over with the result

$$\begin{aligned} \langle t_1 \rangle_l &= -\pi i \Delta \int_{\mathbf{k}} \frac{k_y}{k}\hat{\psi}(-\mathbf{k}) \frac{6\pi T k_c dk_c}{J(2\pi)^2 k_c^2}, \\ \langle t_2 \rangle_l &= 0, \\ \langle t_3 \rangle_l &= 0. \end{aligned} \tag{20}$$

This result implies

$$\Delta' = \Delta - \frac{\Delta T}{\pi J}\frac{dk_c}{k_c}. \tag{21}$$

Defining $dk_c/k_c = dl$, the flow equation results:

$$\frac{d\Delta}{dl} = -\frac{\Delta T}{\pi J}. \tag{22}$$

J is not renormalized to $O(\Delta)$.

The same calculation can be performed for a $s=-1/2$ disclination, using the relation

$$\theta(r,\phi) = -\phi/2 + \psi(r,\phi). \tag{23}$$

The Hamiltonian (2) is expanded in powers of ψ, with the result

$$\begin{aligned} H[\psi] = \frac{J}{2}\int \left(\frac{1}{4r^2} + \psi_x^2 + \psi_y^2\right) + \frac{5\Delta}{4}\int \frac{y^3 - 3x^2 y}{r^5}\psi \\ + \frac{\Delta}{4}\int \left[\frac{5(x^3 - 3xy^2)\psi^2}{r^5} + \frac{2x(\psi_y^2 + \psi_x^2)}{r} + \frac{4y\psi_x\psi_y}{r}\right] \\ + \frac{\Delta}{6}\int \left[\frac{5(3x^2 y - y^3)\psi^3}{r^5} + \frac{6y\psi(\psi_y^2 - \psi_x^2)}{r}\right. \\ \left. - \frac{12x\psi\psi_x\psi_y}{r}\right] + \frac{\Delta}{12}\int \left[\frac{5(3xy^2 - x^3)\psi^4}{r^5}\right. \\ \left. + \frac{12x\psi^2(\psi_y^2 + \psi_x^2)}{r} - \frac{24y\psi^2\psi_x\psi_y}{r}\right]. \end{aligned} \tag{24}$$

The renormalization of Δ is again tracked by integrating out ψ on a momentum shell to first order in T/J and watching how terms from the ψ^3 expression contribute to terms in the ψ expression. The flow equation that results is

$$\frac{d\Delta}{dl} = -\frac{\Delta T}{\pi J}. \tag{25}$$

One can see that Δ renormalizes in the same way about $\pm 1/2$ disclinations. In fact, the same flow equation describes the renormalization of Δ in the absence of disclinations [5].

The renormalization of the coupling J and the disclination fugacity y can be studied with the correlation function approach used for the standard X-Y model [6]. The result, combined with the results above, is

$$\begin{aligned} \frac{dT/J}{dl} &= \pi^3 (y a_0^2)^2 + O(\Delta^2, y^4, y^2\Delta), \\ \frac{d\Delta}{dl} &= -\Delta T/(\pi J) + O(\Delta^2, y^2\Delta), \\ \frac{dy a_0^2}{dl} &= \left(2 - \frac{\pi J}{4T}\right) y a_0^2 + O(y^2\Delta, y^3). \end{aligned} \tag{26}$$

One can see that at the critical point the renormalized coupling is $J_R/T = 8/\pi$. Furthermore, Δ scales as

$$\Delta_R^2 \sim \Delta^2 (\xi/a_0)^{-1/4}, \tag{27}$$

where the correlation length is given by $\xi = a_0 \exp(l)$.

IV. DISCLINATION FREE ENERGIES IN ORDERED PHASE

While the renormalization-group calculations show how Δ becomes irrelevant at the isotropic-ordered transition, they do not directly show how the disclination densities scale near the transition. To estimate the $\pm 1/2$ disclination densities, expressions are needed for the free energies of isolated disclinations. Perturbation theory is here used to calculate directly these free energies in the ordered phase. The results should also be applicable to correlated regions within a macroscopically disordered phase near the isotropic-ordered transition.

The free energy of a disclination will be evaluated to $O(\Delta^2)$. Equation (2) is first integrated by parts with the result

$$\begin{aligned} H = \frac{J}{2}\int dx\, dy\, (\theta_x^2 + \theta_y^2) - \frac{\Delta}{4}\int dx\, dy \sin(2\theta)(\theta_{yy} - \theta_{xx}) \\ - \frac{\Delta}{2}\int dx\, dy \cos(2\theta)\theta_{xy}. \end{aligned} \tag{28}$$

Although θ is discontinuous in the presence of a disclination, the result is the same if Eq. (16) or (23) is used and the integration by parts done in terms of ψ. A cumulant expansion is used for the free energy:

$$F = E_0 + \langle \delta H \rangle_{0c} - \frac{1}{2}\langle (\delta H)^2 \rangle_{0c}/T + \cdots. \tag{29}$$

Here the averages are done with respect to the reference system with Hamiltonian H_0, indicated by subscript zero, and are connected, indicated by subscript c. The functional δH is $H - H_0$. The reference system is chosen to be

$$H_0[\psi] = \frac{J}{2}\int d\mathbf{r}\left(\frac{1}{4r^2} + \psi_x^2 + \psi_y^2\right), \tag{30}$$

where $\theta = s\phi + \psi$.

Specializing to the case of a $s=+1/2$ disclination, the perturbation becomes

$$\begin{aligned} \delta H[\psi] = \int d\mathbf{r}\left[\frac{\Delta y}{4r^3}\sin(2\psi) - \frac{\Delta y}{4r}\cos(2\psi)(\psi_{yy} - \psi_{xx})\right. \\ - \frac{\Delta x}{2r}\cos(2\psi)\psi_{xy} + \frac{\Delta x}{4r^3}\cos(2\psi) - \frac{\Delta x}{4r}\sin(2\psi) \\ \left. \times (\psi_{yy} - \psi_{xx}) + \frac{\Delta y}{2r}\sin(2\psi)\psi_{xy}\right]. \end{aligned} \tag{31}$$

A short calculation shows

$$\langle \delta H \rangle_{0c} = 0. \tag{32}$$

The first nonzero contribution to the free energy is, therefore, $O(\Delta^2)$. The form of Eq. (31), with three terms even in ψ and three terms odd, simplifies the evaluation of $\langle (\delta H)^2 \rangle_{0c}$. Even so, there are 12 Gaussian averages that must be performed. A typical term is

$$\int d\mathbf{r}_1 d\mathbf{r}_2 \langle \cos[2\psi(\mathbf{r}_1)]\psi_{xx}(\mathbf{r}_1)\cos[2\psi(\mathbf{r}_2)]\psi_{xy}(\mathbf{r}_2)\rangle_{0c}$$
$$= 2\int d\mathbf{r}_1 d\mathbf{r}_2 e^{4\chi(r_{12})-4\chi(0)}\left\{[\chi_{xx}(r_{12})-\chi_{xx}(0)][\chi_{xy}(r_{12}) - \chi_{xy}(0)] + \frac{1}{4}\chi_{xxxy}(r_{12})\right\} + 2\int d\mathbf{r}_1 d\mathbf{r}_2 e^{-4\chi(r_{12})-4\chi(0)} \times\left\{-[\chi_{xx}(r_{12})+\chi_{xx}(0)][\chi_{xy}(r_{12})+\chi_{xy}(0)] + \frac{1}{4}\chi_{xxxy}(r_{12})\right\}, \tag{33}$$

where $r_{12}=|\mathbf{r}_1-\mathbf{r}_2|$ and

$$\hat{\chi}(k)=\frac{T}{Jk^2},$$

$$\chi(r)=\frac{T}{2\pi J}\ln(R/r),$$

$$\chi(0)=\frac{T}{2\pi J}\ln(R/a_0). \tag{34}$$

With the definition $z=2T/(\pi J)$, the first integral in Eq. (33) scales like $(R/a_0)^{-z}$ and the second term scales like $(R/a_0)^{-2z}(R/a_0)^{z}$. Both terms must in principle be evaluated. However, all 12 terms that contain the factor $e^{-4\chi(r_{12})-4\chi(0)}$ cancel by $x\leftrightarrow y$ symmetry. The symmetry $\mathbf{r}_1\leftrightarrow\mathbf{r}_2$ is applied to the other 12 terms with the result

$$\int d\mathbf{r}_1 d\mathbf{r}_2 \langle(\delta H)^2\rangle_{0c} = \frac{\Delta^2}{16}\int d\mathbf{r}_1 d\mathbf{r}_2 e^{4\chi(r_{12})}\left[\left\{\frac{y_1}{r_1^3}\frac{y_2}{r_2^3}\right\} + \left\{4\frac{y_1}{r_1}\frac{y_2}{r_2}[\chi_{yy}(r_{12})-\chi_{xx}(r_{12})]^2 + 16\frac{x_1}{r_1}\frac{x_2}{r_2}\chi_{xy}^2(r_{12})\right\} + \left\{\frac{y_1}{r_1}\frac{y_2}{r_2}\nabla^4\chi(r_{12})\right\} + \left\{-4\frac{y_1}{r_1^3}\frac{y_2}{r_2}[\chi_{yy}(r_{12})-\chi_{xx}(r_{12})] - 8\frac{y_1}{r_1^3}\frac{x_2}{r_2}\chi_{xy}(r_{12})\right\}\right] \equiv I_1+I_2+I_3+I_4, \tag{35}$$

with the redefinition $\chi(r_{12})=-(z/4)\ln(r_{12}/a_0)$. The four integrals I_1–I_4 represent integration over the four terms in the curly brackets.

These integrals can now be evaluated. This will be done in Fourier space, and the following Fourier transforms $\mathcal{F}$ will be helpful:

$$\mathcal{F}\{r^{-z}\}=2\pi k^{z-2}\frac{2\Gamma(1-z/2)}{2^z\Gamma(z/2)},$$

$$\mathcal{F}\{y/r^3\}=2\pi i\sin\phi,$$

$$\mathcal{F}\{y/r\}=2\pi i\sin\phi/k^2. \tag{36}$$

The first of these transforms is well defined for $0<z<2$. The relation is valid for all z by analytic continuation from the relation $\mathcal{F}\{\nabla^2 f\}=-k^2\hat{f}(k)$. With these definitions, the first integral becomes

$$I_1=\frac{\Delta^2 a_0^z}{16}\int_{\mathbf{k}}|2\pi i\sin\phi|^2 2\pi k^{z-2}\frac{2\Gamma(1-z/2)}{2^z\Gamma(z/2)} = \frac{\Delta^2\pi^2}{8}\frac{2\Gamma(1-z/2)}{2^z\Gamma(z/2)}\frac{1-(R/a_0)^{-z}}{z} = \frac{\Delta^2\pi^2 z}{8}\frac{\Gamma(1-z/2)(1+z/2)}{2^z\Gamma(2+z/2)}\frac{1-(R/a_0)^{-z}}{z}. \tag{37}$$

The second integral becomes

$$I_2=\frac{\Delta^2 z^2}{16}\int d\mathbf{r}_1 d\mathbf{r}_2\left(\frac{r_{12}}{a_0}\right)^{-z-4}\frac{y_1}{r_1}\frac{y_2}{r_2} = \frac{\Delta^2 z^2 a_0^z}{16}\int_{\mathbf{k}}\left|\frac{2\pi i\sin\phi}{k^2}\right|^2 2\pi k^{z+2}\frac{2\Gamma(-1-z/2)}{2^{4+z}\Gamma(2+z/2)} = \frac{\Delta^2\pi^2 z^2}{8}\frac{2\Gamma(-1-z/2)}{2^{4+z}\Gamma(2+z/2)}\frac{1-(R/a_0)^{-z}}{z} = \frac{\Delta^2\pi^2 z}{32}\frac{\Gamma(1-z/2)}{2^z\Gamma(2+z/2)(1+z/2)}\frac{1-(R/a_0)^{-z}}{z}. \tag{38}$$

The following identity will be useful in evaluating the third integral:

$$\chi(r)=-\frac{z}{4}\lim_{\alpha\to 0}\frac{1-(r/a_0)^{-\alpha}}{\alpha}, \tag{39}$$

which implies

$$\nabla^4\chi(r)=\frac{z}{4}\lim_{\alpha\to 0}\alpha(\alpha+2)^2(r/a_0)^{-\alpha-4}. \tag{40}$$

Using this result, one finds

$$z^{-1}\mathcal{F}\{r^{-z}\nabla^4\chi\}=\frac{1}{4}\lim_{\alpha\to 0}\alpha(\alpha+2)^2\frac{k^4}{(z+\alpha)^2(z+\alpha+2)^2}\times\frac{4\pi k^{z+\alpha-2}\Gamma[1-(z+\alpha)/2]}{2^{z+\alpha}\Gamma[(z+\alpha)/2]} = \begin{cases}\pi k^2/2, & z=0\\ 0, & z\neq 0.\end{cases} \tag{41}$$

The term I_3, therefore, vanishes for nonzero temperatures. It is convenient to break the fourth integral into two parts

$$I_{4a}=\frac{\Delta^2}{4}\int d\mathbf{r}_1 d\mathbf{r}_2 \frac{y_1}{r_1^3}\frac{y_2}{r_2}\left(\frac{r_{12}}{a_0}\right)^{-z}[\chi_{xx}(r_{12})-\chi_{yy}(r_{12})],$$

$$I_{4b}=-\frac{\Delta^2}{2}\int d\mathbf{r}_1 d\mathbf{r}_2 \frac{y_1}{r_1^3}\frac{x_2}{r_2}\left(\frac{r_{12}}{a_0}\right)^{-z}\chi_{xy}(r_{12}). \quad (42)$$

The following trick is used to evaluate these terms:

$$r^{-z}[\chi_{xx}(r)-\chi_{yy}(r)]=\lim_{\alpha\to 0}\frac{z}{4\alpha}r^{-z}(\partial_x^2-\partial_y^2)r^{-\alpha}$$

$$=\frac{z}{2}r^{-z-2}\cos(2\phi). \quad (43)$$

In this form, the Fourier transforms can be evaluated, with the result

$$I_{4a}=\frac{\Delta^2 a_0^z}{4}\int_{\mathbf{k}}\frac{|2\pi i\sin\phi|^2}{k^2}\left(-\frac{\pi z}{2}\right)\cos(2\phi)k^z\frac{\Gamma(1-z/2)}{2^z\Gamma(2+z/2)}$$

$$=\frac{\Delta^2\pi^2 z}{16}\frac{\Gamma(1-z/2)}{2^z\Gamma(2+z/2)}\frac{1-(R/a_0)^{-z}}{z}. \quad (44)$$

Similarly,

$$I_{4b}=-\frac{\Delta^2 a_0^z}{2}\int_{\mathbf{k}}(2\pi i\sin\phi)^*\frac{2\pi i\cos\phi}{k^2}\left(-\frac{\pi z}{4}\right)$$

$$\times\sin(2\phi)k^z\frac{\Gamma(1-z/2)}{2^z\Gamma(2+z/2)}$$

$$=\frac{\Delta^2\pi^2 z}{16}\frac{\Gamma(1-z/2)}{2^z\Gamma(2+z/2)}\frac{1-(R/a_0)^{-z}}{z}. \quad (45)$$

Combining all these results, one finds for the free energy of a $+1/2$ disclination at the origin

$$F_{+1/2}=\frac{\pi J}{4}\ln(R/a_0)-\frac{\pi\Delta^2}{32J}\frac{\Gamma(1-z/2)}{2^z\Gamma(2+z/2)}\left(8+2z+\frac{1}{1+z/2}\right)$$

$$\times\frac{1-(R/a_0)^{-z}}{z}+O(\Delta^3). \quad (46)$$

The ground-state energy is found to be

$$F_{+1/2}\sim\left(\frac{\pi J}{4}-\frac{9\pi\Delta^2}{32J}\right)\ln(R/a_0)+O(\Delta^3)\ \text{ as }\ T\to 0, \quad (47)$$

in agreement with Eq. (11).

For the case of a $s=-1/2$ disclination, the perturbation to consider is

$$\delta H[\psi]=\frac{\Delta}{4}\int d\mathbf{r}\left[\frac{y^3-3x^2y}{r^5}\sin(2\psi)+\frac{y}{r}\cos(2\psi)(\psi_{yy}-\psi_{xx})\right.$$

$$-\frac{2x}{r}\cos(2\psi)\psi_{xy}+\frac{3xy^2-x^3}{r^5}\cos(2\psi)$$

$$\left.-\frac{x}{r}\sin(2\psi)(\psi_{yy}-\psi_{xx})-\frac{2y}{r}\sin(2\psi)\psi_{xy}\right]. \quad (48)$$

A short calculation shows

$$\langle\delta H\rangle_{0c}=0, \quad (49)$$

so that the first nonzero contribution to the free energy is $O(\Delta^2)$. As before, averages that lead to terms with $e^{-4\chi(r_{12})-4\chi(0)}$ cancel by $x\leftrightarrow y$ symmetry. Also as before, the term containing the $\nabla^4\chi(r)$ vanishes at nonzero temperature. After some simplification, one finds

$$\int d\mathbf{r}_1 d\mathbf{r}_2\langle(\delta H)^2\rangle_{0c}=I_2+\frac{\Delta^2}{16}\int d\mathbf{r}_1 d\mathbf{r}_2 e^{4\chi(r_{12})}\left[\{f_1 f_2\}\right.$$

$$+\left\{4f_1\frac{y_2}{r_2}[\chi_{yy}(r_{12})-\chi_{xx}(r_{12})]\right\}$$

$$\left.+\left\{-8f_1\frac{x_2}{r_2}\chi_{xy}(r_{12})\right\}\right], \quad (50)$$

where $f_i=(y_i^3-3x_i^2y_i)/r_i^5$. The result

$$\hat{f}(\mathbf{k})=i\pi\left(-6\sin\phi+8\cos^2\phi\sin\phi+\frac{16}{3}\sin^3\phi\right) \quad (51)$$

will be used.

The integral (50) is split into the three bracketed pieces. The first integral is

$$I_5=\frac{\Delta^2}{16}\int d\mathbf{r}_1 d\mathbf{r}_2\left(\frac{r_{12}}{a_0}\right)^{-z}f_1 f_2$$

$$=\frac{\Delta^2 a_0^z}{16}\int_{\mathbf{k}}|\hat{f}(\mathbf{k})|^2 2\pi k^{z-2}\frac{2\Gamma(1-z/2)}{2^z\Gamma(z/2)}$$

$$=\frac{\Delta^2\pi^2 z}{72}\frac{\Gamma(1-z/2)(1+z/2)}{2^z\Gamma(2+z/2)}\frac{1-(R/a_0)^{-z}}{z}. \quad (52)$$

The second integral is

$$I_6=\frac{\Delta^2}{16}\int d\mathbf{r}_1 d\mathbf{r}_2\left(\frac{r_{12}}{a_0}\right)^{-z}4f_1\frac{y_2}{r_2}[\chi_{yy}(r_{12})-\chi_{xx}(r_{12})]$$

$$=\frac{\Delta^2 a_0^z}{4}\int_{\mathbf{k}}\hat{f}^*(\mathbf{k})\frac{2\pi i\sin\phi}{k^2}\frac{\pi z}{2}\cos(2\phi)k^z\frac{\Gamma(1-z/2)}{2^z\Gamma(2+z/2)}$$

$$=\frac{\Delta^2\pi^2 z}{48}\frac{\Gamma(1-z/2)}{2^z\Gamma(2+z/2)}\frac{1-(R/a_0)^{-z}}{z}. \quad (53)$$

The third integral is

$$I_7=\frac{\Delta^2}{16}\int d\mathbf{r}_1 d\mathbf{r}_2\left(\frac{r_{12}}{a_0}\right)^{-z}\left(-8f_1\frac{x_2}{r_2}\right)\chi_{xy}(r_{12})$$

$$=-\frac{\Delta^2 a_0^z}{2}\int_{\mathbf{k}}\hat{f}^*(\mathbf{k})\frac{2\pi i\cos\phi}{k^2}\left(-\frac{\pi z}{4}\right)$$

$$\times\sin(2\phi)k^z\frac{\Gamma(1-z/2)}{2^z\Gamma(2+z/2)}$$

$$=\frac{\Delta^2\pi^2 z}{48}\frac{\Gamma(1-z/2)}{2^z\Gamma(2+z/2)}\frac{1-(R/a_0)^{-z}}{z}. \quad (54)$$

Combining all these results, one finds for the free energy of a $-1/2$ disclination at the origin

$$F_{-1/2}=\frac{\pi J}{4}\ln(R/a_0)-\frac{\pi\Delta^2}{288J}\frac{\Gamma(1-z/2)}{2^z\Gamma(2+z/2)}\times\left(16+2z+\frac{9}{1+z/2}\right)\frac{1-(R/a_0)^{-z}}{z}+O(\Delta^3). \tag{55}$$

The ground-state energy is given by

$$F_{-1/2}\sim\left(\frac{\pi J}{4}-\frac{25\pi\Delta^2}{288J}\right)\ln(R/a_0)+O(\Delta^3)\ \text{ as }\ T\to 0, \tag{56}$$

in agreement with Eq. (13).

The difference in free energies of $\pm 1/2$ disclinations is, therefore, given by

$$F_{+1/2}-F_{-1/2}=\frac{\pi\Delta^2}{J}\frac{\Gamma(1-z/2)}{2^z\Gamma(2+z/2)}\frac{7+2z}{36}\frac{1-(R/a_0)^{-z}}{z}+O(\Delta^3). \tag{57}$$

Near the isotropic-ordered transition, the coupling renormalizes to $z_R=1/4$ and $J_R/T=8/\pi$, so one finds

$$(F_{+1/2}-F_{+1/2})/T\sim-0.8891(\Delta/T)^2[1-(\xi/a_0)^{-1/4}]+[E_{c_{+1/2}}(\Delta)-E_{c_{-1/2}}(\Delta)]/T \quad \text{as}\ \ \xi\to\infty. \tag{58}$$

Additional microscopic core energies that may be distinct for the two different disclinations have been explicitly added in this equation. By comparing Eq. (58) with Eqs. (11), (13), and (27), one sees that the appropriate finite-size scaling replacement is $\Delta_R^2\ln(R/a_0)\to\Delta^2[1-(R/a_0)^{-z}]/z$. This relation gives a very good approximation to Eq. (58).

V. DISCLINATION DENSITIES IN THE ISOTROPIC PHASE

The disclination density in the isotropic phase is calculated in this section, taking into account interactions between disclinations. In the isotropic phase, the free energy can be expressed in terms of the order parameter [7]

$$Q=Q_0\begin{pmatrix}n_x^2-n_y^2 & 2n_xn_y\\ 2n_xn_y & n_y^2-n_x^2\end{pmatrix}=Q_0\begin{pmatrix}\cos(2\theta) & \sin(2\theta)\\ \sin(2\theta) & -\cos(2\theta)\end{pmatrix}\equiv\begin{pmatrix}q_1 & q_2\\ q_2 & -q_1\end{pmatrix}. \tag{59}$$

An expression that reduces to Eq. (2) in the low-temperature, fixed-Q_0 phase is

$$H=\frac{m}{4}\sum_{i,j}\int d\mathbf{r}Q_{ij}^2+\frac{j_1}{4}\sum_{i,j,k}\int d\mathbf{r}(\partial_iQ_{jk})^2+j_2\sum_{i,j,s,t}\int d\mathbf{r}Q_{si}Q_{tj}\partial_s\partial_tQ_{ij}, \tag{60}$$

where $j_1=J/4Q_0^2$ and $j_2=\Delta/16Q_0^3$. Expressed in terms of the unique components q_1 and q_2, the Hamiltonian becomes

$$H=\frac{m}{2}\int d\mathbf{r}(q_1^2+q_2^2)+\frac{j_1}{2}\int d\mathbf{r}(q_{1x}^2+q_{1y}^2+q_{2x}^2+q_{2y}^2)+\delta H, \tag{61}$$

where

$$\delta H=j_2\int d\mathbf{r}[q_1^2(q_{1xx}-q_{1yy})+q_2^2(q_{1yy}-q_{1xx})+2q_1q_2(q_{2xx}-q_{2yy})+4q_1q_2q_{1xy}+2q_2^2q_{2xy}-2q_1^2q_{2xy}]. \tag{62}$$

The vector field $\mathbf{q}=(q_1,q_2)$ will have disclinations of strength ± 1 when the θ field has disclinations of strength $\pm 1/2$. The density of disclinations can be written as [8]

$$\rho(\mathbf{r})=\frac{1}{2}\sum_l\ \mathrm{sgn}[\det\partial_iq_j(\mathbf{r})]\,\delta(\mathbf{r}-\mathbf{r}_l), \tag{63}$$

where $\mathbf{q}(\mathbf{r}_l)=\mathbf{0}$. This expression can be simplified as

$$\rho(\mathbf{r})=\frac{1}{2}\delta(\mathbf{q})\det\partial_iq_j(\mathbf{r})=\frac{1}{2}\delta(q_1)\delta(q_2)(q_{1x}q_{2y}-q_{1y}q_{2x}). \tag{64}$$

Furthermore, the number density is given by

$$|\rho(\mathbf{r})|=\frac{1}{2}\delta(q_1)\delta(q_2)|q_{1x}q_{2y}-q_{1y}q_{2x}|. \tag{65}$$

These densities will be evaluated by perturbation theory in Δ. The reference system will be Eq. (61), with $\delta H=0$. It is clear that q_1 and q_2 are independent Gaussian fields with the correlation function $\chi_0(r)=T/(2\pi j_1)K_0(r/\xi)$, where the correlation length is given by $\xi=(j_1/m)^{1/2}$. Averages that involve the factor $\delta(q_1)$ will occur. This factor can essentially be absorbed into the Gaussian weight with the trick

$$\langle\delta(q(\mathbf{0}))f[q]\rangle_0=\frac{\int\mathcal{D}[q]P[q]\delta(q(\mathbf{0}))f[q]}{\int\mathcal{D}[q]P[q]}=\frac{\int\mathcal{D}[q]P[q]\delta(q(\mathbf{0}))f[q]}{\int\mathcal{D}[q]P[q]\delta(q(\mathbf{0}))}\times\frac{\int\mathcal{D}[q]P[q]\delta(q(\mathbf{0}))}{\int\mathcal{D}[q]P[q]}, \tag{66}$$

where $P[q]\mathcal{D}[q]$ is the probability of a given field configuration. This result is defined to be

$$\langle f[q]\rangle_\delta\langle\delta(q(\mathbf{0}))\rangle_0=[2\pi\chi_0(0)]^{-1/2}\langle f[q]\rangle_\delta. \tag{67}$$

It turns out that the weight $P[q]\delta(q(\mathbf{0}))$ still implies that q is a Gaussian field, but with the new correlation function [9–11]

$$\langle q(\mathbf{r}_1)q(\mathbf{r}_2)\rangle_\delta \equiv \chi(\mathbf{r}_1,\mathbf{r}_2)=\chi_0(|\mathbf{r}_1-\mathbf{r}_2|) - \chi_0(r_1)\chi_0(r_2)/\chi_0(0). \tag{68}$$

The average number density of disclinations in the limit $\Delta\to 0$ is first evaluated. The following term will arise:

$$\langle \delta(q_1(\mathbf{0}))\delta(q_2(\mathbf{0}))|q_{1x}(\mathbf{0})q_{2y}(\mathbf{0})-q_{1y}(\mathbf{0})q_{2x}(\mathbf{0})|\rangle_0 = [2\pi\chi_0(0)]^{-1}\langle |q_{1x}(\mathbf{0})q_{2y}(\mathbf{0})-q_{1y}(\mathbf{0})q_{2x}(\mathbf{0})|\rangle_\delta. \tag{69}$$

Using Eq. (68), one can see that all of the variables in this average are independently Gaussian, with variance $\gamma=-\chi_{0xx}(0)=-\chi_{0yy}(0)=-\chi_{0rr}(0)$. The probability distribution for $P(q_{1x}q_{2y}=x)$ is $K_0(x/\gamma)/(\pi\gamma)$, and the probability distribution for $P(q_{1x}q_{2y}-q_{1y}q_{2x}=y)$ is $\exp(-|y|/\gamma)/2\gamma$. With this result the average can be carried out

$$2\langle|\rho|\rangle=\frac{-\chi_{0rr}(0)}{2\pi\chi_0(0)}+O(\Delta). \tag{70}$$

The effect of nonzero Δ on the average disclination asymmetry is now evaluated. From Sec. IV, one knows that the essential effect of nonzero Δ is to create distinct core energies for $+1/2$ and $-1/2$ disclinations. This effect is modeled by replacing Eq. (62) with

$$\delta H=-2\int d\mathbf{r}\mu(r)\rho(\mathbf{r}). \tag{71}$$

The parameter μ is related to the core energy difference and there will be a unique mapping from Δ^2 to μ for small Δ. The core energy difference is considered to be nonzero and constant within a large region of radius R inside a macroscopically large system. This is done because the macroscopic disclination asymmetry is identically zero for a system with the periodic boundary conditions implied by the Fourier analysis. A grand canonical ensemble with a fluctuating disclination asymmetry arises when considering a region of the periodic system. The disclination asymmetry is now calculated for small μ:

$$\langle\rho(\mathbf{0})\rangle=\langle\rho(\mathbf{0})\rangle_0+2\mu\int_{r<R}d\mathbf{r}\langle\rho(\mathbf{0})\rho(\mathbf{r})\rangle_{0c}+O(\mu^2). \tag{72}$$

The disclination asymmetry is seen to be related to the disclination correlation function by a fluctuation-dissipation theorem. The disclination correlation function is given by [8]

$$4\langle\rho(\mathbf{0})\rho(\mathbf{r})\rangle_0=2\langle|\rho|\rangle_0+g_0(r), \tag{73}$$

where the δ function comes from the self-terms in the average, and $g_0(r)$ is a radially symmetric function that accounts for correlations between distinct disclinations. To calculate $g_0(r)$ the same trick as before is used. One has

$$\langle\delta(q(\mathbf{0}))\delta(q(\mathbf{r}))\rangle_0=\frac{1}{2\pi[\chi_0^2(0)-\chi_0^2(r)]^{1/2}}. \tag{74}$$

The field correlation function is now given by [11]

$$\chi(\mathbf{r}_1,\mathbf{r}_2)=\chi_0(|\mathbf{r}_1-\mathbf{r}_2|)-[\chi_0(r_1)\chi_0(r)\chi_0(r_2) - \chi_0(r_1)\chi_0(r)\chi_0(|\mathbf{r}_2-\mathbf{r}|) - \chi_0(|\mathbf{r}_1-\mathbf{r}|)\chi_0(r)\chi_0(r_2)+\chi_0(|\mathbf{r}_1-\mathbf{r}|)\chi_0(r) \times\chi_0(|\mathbf{r}_2-\mathbf{r}|)][\chi_0^2(0)-\chi_0^2(r)]^{-1}. \tag{75}$$

This form implies

$$\langle q_{1\alpha}(\mathbf{0})q_{1\beta}(\mathbf{r})\rangle_\delta=-\chi_{0\alpha\beta}(r)-\chi_{0\alpha}(r)\chi_0(r)\chi_{0\beta}(r)/[\chi_0^2(0) - \chi_0^2(r)]. \tag{76}$$

With these results one finds

$$g_0(r)=\frac{1}{2\pi^2 r[\chi_0^2(0)-\chi_0^2(r)]}\left[\chi_{0r}(r)\chi_{0rr}(r) + \frac{\chi_0(r)\chi_{0r}^3(r)}{\chi_0^2(0)-\chi_0^2(r)}\right]. \tag{77}$$

Per Eq. (72) this result will be integrated over r. The first term can be integrated by parts, with the result

$$\int d\mathbf{r}g_0(r)=\lim_{r\to 0}\frac{\chi_{0r}(r)}{2\pi r\chi_0(0)}=-2\langle|\rho|\rangle_0. \tag{78}$$

This result, along with Eqs. (72) and (73), implies that the densities of $+1/2$ and $-1/2$ disclinations remain equal even in the presence of distinct core energies. A more careful conclusion is that the average disclination density is zero within the bulk region. It can be nonzero near the boundary because the integral in Eq. (72) will be cut off before $g_0(r)$ is negligible. This contribution is estimated to be

$$\langle n_{+1/2}-n_{-1/2}\rangle=2\mu\int_{r,r'<R}d\mathbf{r}d\mathbf{r}'\langle\rho(\mathbf{r})\rho(\mathbf{r}')\rangle_0+O(\mu^2) \approx 2\pi\mu R\xi\langle|\rho|\rangle/2 \sim c[\exp(-\beta E_{c_{+1/2}})-\exp(-\beta E_{c_{-1/2}})] \times R/\xi \text{ as } \xi\ll R\to\infty. \tag{79}$$

The scaling $\langle|\rho|\rangle\sim c\xi^{-2}$ has been used. It arises because the disorder created by unbound disclinations defines the correlation length.

VI. MONTE CARLO CALCULATIONS ON A LATTICE MODEL

This section describes both a lattice model for nematics with unequal Frank constants and a Monte Carlo procedure for evaluating the properties of the model. The fundamental degrees of freedom are spins of unit length on a square lattice. The Hamiltonian has both nearest- and next-nearest-neighbor couplings:

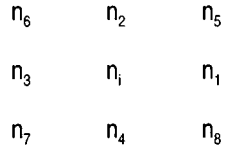

FIG. 4. Definition of spins used in Hamiltonian (80).

$$H=\frac{J}{4}\sum_i \sum_{j<5}[1-(\mathbf{n}_i\cdot\mathbf{n}_j)^2]+\frac{\Delta}{8}\sum_i \sum_{j<5}(-1)^j \times[1-(\mathbf{n}_i\cdot\mathbf{n}_j)^2][n_{ix}^2+n_{jx}^2-n_{iy}^2-n_{jy}^2] + \frac{\Delta}{8}\sum_i \sum_{4<j<9}(-1)^j[1-(\mathbf{n}_i\cdot\mathbf{n}_j)^2][n_{ix}n_{iy}+n_{jx}n_{jy}]. \tag{80}$$

The sum over i is over sites on a square lattice. The sum over $j=1$ to 8 is defined according to Fig. 4. Terms that would place j off the lattice are ignored. This Hamiltonian satisfies the symmetry $\mathbf{n}_i\leftrightarrow-\mathbf{n}_i$. The couplings between spins are symmetric under the interchange $\mathbf{n}_i\leftrightarrow\mathbf{n}_j$. Finally, in the limit of a very small lattice spacing, Eq. (80) reduces to Eq. (2). Numerical values of Eq. (80) agree with those from Eqs. (3) and (4) for specific forms of the θ field.

This model will be equilibrated with a simple Metropolis move that perturbs individual spins. Specifically, a vector randomly distributed in a disk of radius r is added to a randomly chosen spin. A value $r=10$ will be found to be satisfactory. The new spin is then normalized to unit length. If the energy of the lattice is lowered by using this new spin, the new spin is adopted. Otherwise, the new spin is adopted with a probability $\exp[(E_o-E_n)/T]$. This move satisfies detailed balance, and so this Monte Carlo procedure will sample the Boltzmann distribution [12]. A natural unit of equilibration time, the Monte Carlo step (MCS), is N^2 iterations of this move on a $N\times N$ lattice. Most runs last for 800 000 MCS after an initial equilibration of 80 000 MCS. For the case of $\Delta=2$, 3 200 000 MCS are performed after an equilibration time of 320 000 MCS. The properties of the lattice are sampled every 50 MCS.

The number of disclinations can be counted by looking at all $(N-1)^2$ plaquettes on the lattice and determining whether a disclination of strength $+1/2$, $-1/2$, or 0 is present at each plaquette. This determination is made by first defining $\mathbf{n}_1$-$\mathbf{n}_4$ to be a counterclockwise ordering of the spins around the plaquette. Double-headed spins are converted into single-headed spins by $m_{ix}=n_{ix}^2-n_{iy}^2$ and $m_{iy}=2n_{ix}n_{iy}$. The following angle is defined for the plaquette:

$$t=\theta_{21}+\theta_{32}+\theta_{43}+\theta_{14}, \tag{81}$$

where $\theta_{ij}=\theta_i-\theta_j$ is constrained to be in the range $(-\pi,\pi)$, and θ_i is the angle associated with spin $\mathbf{m}_i$. The disclination density at this plaquette is defined by

$$s=\frac{t}{4\pi}. \tag{82}$$

The disclination asymmetry is equal to the sum of this density over the entire lattice. By the analog of Green's theorem, it can be written as a sum of θ_{ij} over the boundary of the lattice.

The correlation length and the correlation time will be measured during a Monte Carlo run to monitor convergence. The position correlation function is defined as

$$g(\mathbf{r})=N^{-2}\sum_{\mathbf{x}}\{[\mathbf{n}(\mathbf{x})\cdot\mathbf{n}(\mathbf{x}-\mathbf{r})]^2-1/2\}, \tag{83}$$

where the $\mathbf{r}$ and $\mathbf{x}$ are integer vectors on the $N\times N$ square lattice. Free boundary conditions imply that there will be significant effects of the boundary in this correlation function. The correlation length is defined in terms of the position correlation function by

$$\xi=\int d\mathbf{r}rg(\mathbf{r}) \Big/ \int d\mathbf{r}g(\mathbf{r}). \tag{84}$$

Here $|\mathbf{r}|$ ranges from 0 to $2^{1/2}N$. Fast Fourier transforms will be used to compute this quantity in $O(N^2\ln^2 N)$ time [13]. The time correlation function is defined as

$$f(t)=\sum_{t'}\mathbf{m}(t')\cdot\mathbf{m}(t'-t), \tag{85}$$

where the $\mathbf{m}(t)=\Sigma_{\mathbf{x}}\mathbf{m}(\mathbf{x},t)$ is the vector sum of the single-headed spins at MCS t. A correlation time could be defined by analogy with Eq. (84), but noise in $f(t)$ for large t causes this approach to be unsatisfactory. Instead, the correlation time τ is defined by the smallest value of τ for which $f(\tau)/f(0)<1/e$.

The interesting observable is the asymmetry between the number of $+1/2$ and $-1/2$ disclinations. This asymmetry will be small, and it will be important to quantify the statistical error in this observable. The difference $\delta n=n_{+1/2}-n_{-1/2}$ must scale as N/ξ by Green's theorem. The variance of this observable should scale with the observable and inversely with the number of independent samplings:

$$\sigma_{\delta n}=c\left[\frac{N/\xi}{T/\tau}\right]^{1/2}, \tag{86}$$

where T is the total number of MCS. This variance is independent of Δ for small Δ, and so the constant c can be determined from the case where $\Delta=0$. In this limit, the values of τ and ξ can also be determined from the case $\Delta=0$.

Figure 5 shows the correlation length as a function of temperature for various lattice sizes. The correlation length grows at lower temperatures. It saturates at a fraction of the lattice size for even lower values of the temperature. The isotropic-ordered transition temperature can be identified by the inflection point of this curve. Finite-size scaling can be used to extrapolate the inflection point as a function of $1/N$ to $N\to\infty$. The result is approximately $J_R/T=4$. Figure 6 shows the correlation time, in units of 50 MCS, as a function of temperature for various lattice sizes. This time also grows for lower temperatures and larger lattices. In fact, near the critical point, the expected scaling $\tau\sim c\xi^2$ is observed.

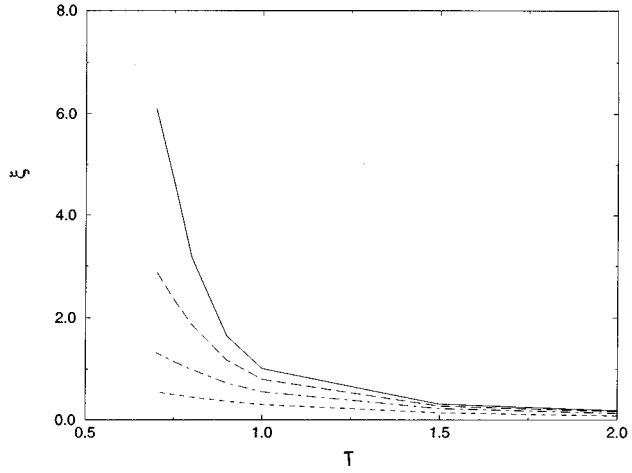

FIG. 5. Correlation length as a function of temperature for the case $J=3$, $\Delta=0$, and $N=4$ (short-dashed line), 8 (dot-dashed line), 16 (long-dashed line), and 32 (solid line).

Figure 7 shows the observed number of disclinations as a function of temperature for various lattice sizes. As expected, the number of disclinations decreases with decreasing temperature. These curves should converge to a universal curve in the limit $N\rightarrow\infty$. This curve is the total number of disclinations, both bound and unbound, so it does not go to zero at the critical point. The curves for different N, however, do intersect at a unique value of J/T. This value can be extrapolated as a function of $1/N$ to $N\rightarrow\infty$ to determine the true critical point. The result is $J_R/T=3.4$. This observable appears to produce a more reliable critical point than does the correlation length.

Not shown are the correlation length and disclination densities for nonzero Δ. The dominant dependence on Δ was through Δ^2. Nonzero values of Δ increased the density of disclinations and decreased the correlation length and time. Furthermore, analysis showed that the observed disclination density scaled like $\rho\sim c\xi^{-2}$, at least for large T, where the disclinations were unpaired. These qualitative effects are consistent with Eqs. (46) and (55).

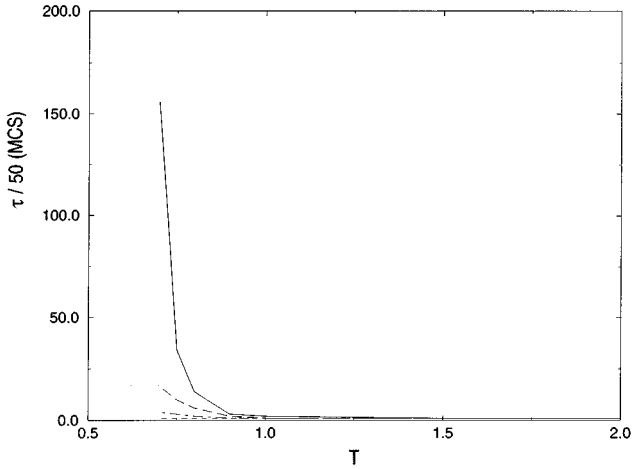

FIG. 6. Correlation time as a function of temperature for the case $J=3$, $\Delta=0$, and $N=4$ (short-dashed line), 8 (dot-dashed line), 16 (long-dashed line), and 32 (solid line).

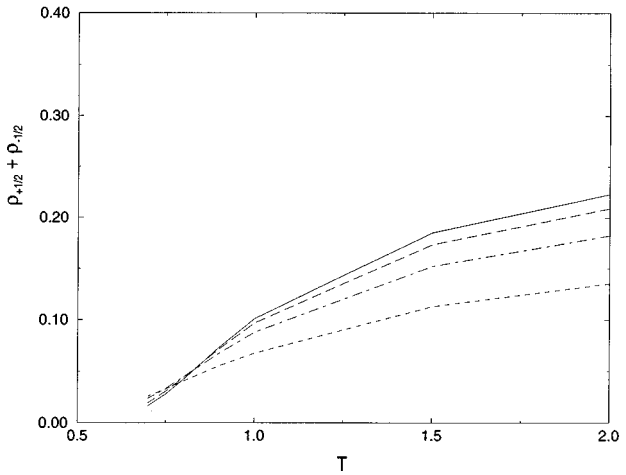

FIG. 7. Disclination density as a function of temperature for the case $J=3$, $\Delta=0$, and $N=4$ (short-dashed line), 8 (dot-dashed line), 16 (long-dashed line), and 32 (solid line).

The limitation of a finite-size lattice prevents the true scaling of the disclination asymmetry near the isotropic-ordered transition from being observed. One can, however, observe the asymmetry for these finite-size systems. Figure 8 shows the asymmetry function $\rho_{+1/2}-\rho_{-1/2}$ for $\Delta=2$ for various lattices sizes. Figure 9 shows the analogous results for $\Delta=3$. This observable can be extrapolated as a function of $1/N$ to $N\rightarrow\infty$ to estimate the behavior for infinite systems. It is clear that the extrapolated result is zero, within statistical error. In fact, one can see that the disclination number asymmetry scales only with the circumference of the system.

VII. DISCUSSION

We see that there is a statistical symmetry in this model. This symmetry enforces $\rho_{+1/2}+\rho_{-1/2}=0$ in the limit of a large system size, even in the presence of nonzero Δ. This symmetry arises because the disclination number asymmetry

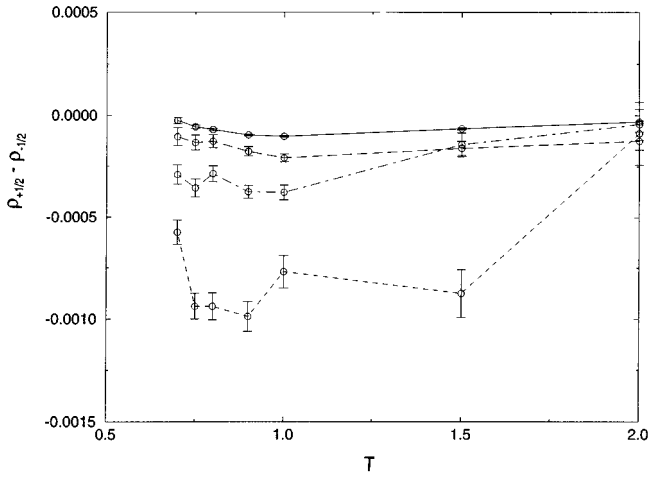

FIG. 8. Disclination asymmetry as a function of temperature for the case $J=3$, $\Delta=2$, and $N=4$ (short-dashed line), 8 (dot-dashed line), 16 (long-dashed line), and 32 (solid line). The error bars are $\pm$ one standard deviation.

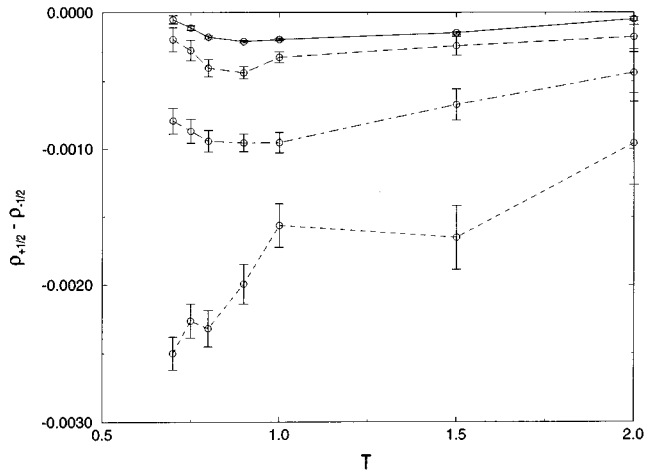

FIG. 9. Disclination asymmetry as a function of temperature for the case $J=3$, $\Delta=3$, and $N=4$ (short-dashed line), 8 (dot-dashed line), 16 (long-dashed line), and 32 (solid line). The error bars are $\pm$ one standard deviation.

can be written as an integral of bounded terms over the periphery of the system, by Green's theorem. This relation, in turn, means that the disclination number asymmetry can scale at most with the linear size of the system. Indeed, this scaling was observed in the Monte Carlo calculations. With a definition of disclinations not susceptible to Green's theorem, this statistical symmetry would not be present. In this case, one would generally expect the disclination asymmetry to scale with N^2/ξ^2 instead of N/ξ.

There are many parallels between the problem of a nematic liquid crystal with unequal Frank constants and a hexatic membrane [14,15]. Disclinations mediate a melting transition in both cases, and the disclination free energy is logarithmic in the correlation length in both cases. For the nematic, unequal Frank constants cause the free energies of $+1/2$ and $-1/2$ disclinations to differ. They only differ by a core energy, however, due to the renormalization of Δ. For the membrane, local buckling causes the free energies of five-fold and sevenfold disclinations to differ. They, too, only differ by a core energy, due to renormalization of the membrane rigidity. As with nematic liquid crystals, there is a topological theorem that relates the number of fivefold and sevenfold disclinations to an integral over a boundary [16]. The natural way for this to happen is $n_5-n_7\sim cR/\xi_A$, where ξ_A is now the hexatic correlation length. The prefactor again depends on the difference between exponentials of core energies. It seems, then, that within the liquid phase of a membrane with hexatic symmetry, differing core energies simply renormalize the line tension and Gaussian rigidity. Near the liquid to hexatic transition, however, constraints imposed by a non-Euclidean membrane geometry frustrate the formation of hexatic order. The system can relieve this frustration by flattening the membrane. One might expect, for example, that the preferred size of a vesicle undergoing a hexatic to liquid transition should scale like the hexatic correlation length. This conjecture is a worthy subject of future calculations.

ACKNOWLEDGMENTS

It is a pleasure to acknowledge discussions with David Nelson and Georg Foltin. This research was supported by the National Science Foundation through Grant Nos. DMR-9417047 and CHE-9403114 and through the MRSEC program through Grant No. DMR-9400396.

[1] P. G. de Gennes and J. Prost, *The Physics of Liquid Crystals*, 2nd ed. (Clarendon, New York, 1993).
[2] J. M. Kosterlitz and D. J. Thouless, J. Phys. C **6**, 1181 (1973).
[3] I. E. Dzyaloshinski, Zh. Eksp. Teor. Fiz. **58**, 1443 (1970) [Soviet Phys. JETP **31**, 773 (1970)].
[4] S. D. Hudson and E. L. Thomas, Phys. Rev. Lett. **62**, 1993 (1989).
[5] D. R. Nelson and R. A. Pelcovits, Phys. Rev. B **16**, 2191 (1977).
[6] D. R. Nelson, in *Phase Transitions and Critical Phenomena*, edited by C. Domb and J. Lebowitz (Academic, New York, 1983), Vol. 7.
[7] D. C. Wright and N. D. Mermin, Rev. Mod. Phys. **61**, 385 (1989).
[8] B. I. Halperin, in *Physics of Defects*, edited by R. Balian, M. Kleman, and J.-P. Poirier (North-Holland, Amsterdam, 1981).
[9] H. Li and M. Kardar, Phys. Rev. Lett. **67**, 3275 (1991).
[10] H. Li and M. Kardar, Phys. Rev. A **46**, 6490 (1992).
[11] D. Chandler, Phys. Rev. E **48**, 2898 (1993).
[12] M. H. Kalos and P. A. Whitlock, *Monte Carlo Methods* (Wiley, New York, 1986), Vol. I.
[13] W. H. Press, B. P. Flannery, S. A. Teukolsky, and W. T. Vetterling, *Numerical Recipes in Fortran*, 2nd ed. (Cambridge Univeristy Press, New York, 1992).
[14] M. W. Deem and D. R. Nelson, Phys. Rev. E **53**, 2551 (1996).
[15] J.-M. Park and T. C. Lubensky, J. Phys. (France) I **6**, 493 (1996).
[16] F. David, in *Statistical Mechanics of Membranes and Surfaces*, edited by D. Nelson, T. Piran, and S. Weinberg (World Scientific, Singapore, 1989).